Space-Time Characteristics of the Wall Shear-Stress Fluctuations in an Axial Turbulent Boundary Layer with Transverse Curvature

Dongshin Shin*
Department of Mechanical System Design Engineering, College of Engineering, Hongik University, Seoul 121-791, Korea
Seungbae Lee
Department of Mechanical Engineering, College of Engineering, Inha University, Incheon 402-751, Korea
Yang Na
CAESIT, Department of Mechanical Engineering, Konkuk University, Seoul 143-701, Korea

Direct numerical simulation database of an axial turbulent boundary layer is used to compute frequency and wave number spectra of the wall shear-stress fluctuations in a low-Reynolds number axial turbulent boundary layer. One-dimensional and two-dimensional power spectra of flow variables are calculated and compared. At low wave numbers and frequencies, the power of streamwise shear stress is larger than that of spanwise shear stress, while the powers of both stresses are almost the same at high wave numbers and frequencies. The frequency/streamwise wave number spectra of the wall flow variables show that large-scale fluctuations to the rms value is largest for the streamwise shear stress, while that of small-scale fluctuations to the rms value is largest for pressure. In the two-point auto-correlations, negative correlation occurs in streamwise separations for pressure, and in spanwise correlation for both shear stresses.

Key Words : Turbulent Boundary Layer, Transverse Curvature, Direct Numerical Simulation

Nomenclature

a : Radius of infinite cylinder
C_f : Friction Coefficient
L : Length of the cylinder
Re : Reynolds Numver
u_τ : Friction Velocity
δ : Boundary layer thickness
τ : Wall shear stress
Φ : Power spectrum

Superscripts
$+$: Wall unit

Subscripts
w : Wall

* Corresponding Author,
E-mail : dsshin@hongik.ac.kr
TEL : +82-2-320-1477; **FAX** : +82-2-324-8911
Department of Mechanical System Design Engineering, College of Engineering, Hongik University, Seoul 121-791, Korea. (Manuscript **Received** May 23, 2005; **Revised** July 11, 2005)

1. Introduction

The behavior of fluctuations of the wall flow variables in a turbulent boundary layer with transverse curvature is of fundamental importance in many practical applications involving flow-induced noise. In flow-induced noise research, it is very important to know the space-time characteristics of the wall pressure and shear-stress fluctuations because they are closely related to the generation of dipole noise (Blake, 1986).

The instantaneous wall pressure and shear stresses are signatures of the phenomena occurring above the wall, and thus there have been

many studies of the behavior of the wall flow variables for a flat turbulent boundary layer (Choi and Moin, 1990) as well as an axial turbulent boundary layer (Neves et al., 1994). Most of them, however, have focused on the wall pressure fluctuations in turbulent boundary layers, and relatively few detailed measurements of the wall shear-stress fluctuations have been made. The scaling law in the wall pressure power spectrum and the functional dependence of p_{wrms}/τ_w on the Reynolds number are relatively well established (Choi and Moin, 1990; Farabee and Casarella, 1991). Recently et al.(1999) reported the space-time characteristics of the wall shear-stress fluctuations in a channel flow but there is almost no consensus on the scaling laws for the wall shear-stress power spectrum and the functional dependence of τ_{1rms}/τ_w on the Reynolds number for an axial turbulent boundary layer with transverse curvature, even though several measurements of the wall shear stress have been made (Wietrzak and Lueptow, 1994; Alfredsson et al., 1988). Here, p_w is the wall pressure fluctuations, $\tau_1=\mu\partial u'/\partial y|_w$ is the wall shear-stress fluctuations, $\tau_w=\mu\partial\bar{u}/\partial y|_w$ is the mean shear stress on the wall, and u' is the streamwise velocity fluctuations. Accurate measurements of the wall shear-stress fluctuations are made difficult by the problems associated with spatial resolution and frequency response of the probe and also with heat conduction to the wall. In general, the complete wall shear-stress spectral data needed for the above mentioned research efforts are still lacking.

The main objective of this work is to compute the complete (three-dimensional) wall shear-stress spectra, as a function of streamwise and spanwise wavenumbers and frequency, using data from direct numerical simulation of turbulent boundary layer with transverse curvature (Shin, 2000).

2. Numerical Method

The governing equations for an incompressible flow are

$$\frac{\partial u_i}{\partial x_i}=0 \tag{1}$$

$$\frac{\partial u_i}{\partial t}+\frac{\partial u_i u_j}{\partial x_j}=-\frac{\partial p}{\partial x_i}+\frac{1}{Re}\frac{\partial^2 u_i}{\partial x_j \partial x_j} \tag{2}$$

where x_i are the coordinates, and u_i are the corresponding velocity components. We developed the code using generalized coordinates in 1 and 2 directions and Cartesian coordinates in the 3 direction. All variables are non-dimensionalized by the boundary layer thickness δ^* and the free-stream velocity u_∞, and Re is the Reynolds number, $Re=u_\infty\delta^*/\nu$, where ν is the kinematic viscosity.

The time integration method used to solve Eqs. (1) and (2) is based on a fully implicit, fractional step method (Choi and Moin, 1990; Kim and Choi, 2004). All the spatial derivatives are approximated with the second order central difference method. We performed direct numerical simulations of axial turbulent boundary layers with spanwise curvature. The details of the direct numerical simulation can be referred in Shin (2000).

In order to study the effects of curvature on a axial turbulent boundary layer, we considered three bounadary layer thicknesses, $\delta/a=2$, 5 and 10. We used a computational mesh with $64\times 95\times 192$ nodes for $\delta/a=2$, 5 and $128\times 95\times 320$ nodes for $\delta/a=10$. The meshes for the axial and circumferential directions are uniform and the ones for the normal direction are generated from hyperbolic tangent function.

3. Computation of the Frequency Spectrum

The power spectrum as a function of the frequency is calculated using the same method as in Choi and Moin (1990). The fully developed axial turbulent boundary layer flow fields with transverse curvature that was previously simulated by Shin (2000) are used as the data base. We considered 4,992 as the total time step with the computational time step of $\Delta t'=1.47\times 10^{-3}\ \delta/u_\tau$, $1.705\times 10^{-3}\delta/u_\tau$ and $1.28\times 10^{-3}\delta/u$ for $\delta/a=2$, 5 and 10, respectively. The shear stresses

and pressure at the cylinder surface are stored every two steps and thus the sampling resolution is $\Delta t=2.94\times10^{-3}\delta/u_\tau$, $3.41\times10^{-3}\delta/u_\tau$ and $2.56\times10^{-3}\delta/u$ for $\delta/a=2$, 5 and 10, respectively. They correspond to $\Delta t^+=0.490$, 0.659 and 0.557 in wall units. The total record of $N=2496$ time samples, covering $T_N=7.34\delta/u_\tau$, $8.51\delta/u_\tau$ and $6.38\delta/u_\tau$ for $\delta/a=2$, 5 and 10, respectively, is divided into $m=12$ over lapping segments (with 50% overlap), each containing $M=2N/(m+1)=384$ points. The resulting resolved frequency range is $0\le\omega\le1068u_\tau\delta$, $0\le\omega\le916u_\tau/\delta$ and $0\le\omega\le1231u_\tau/\delta$ for $\delta/a=2$, 5 and 10, respectively. Their frequency resolutions are $\Delta\omega=5.57u_\tau/\delta$, $\Delta\omega=4.55u_\tau/\delta$ and $\Delta\omega=6.41u_\tau/\delta$ for $\delta/a=2$, 5 and 10, respectively.

The shear-stress fluctuations at the wall, $\tau_1(x, z, t)=\mu\partial u'/\partial y|_w$ and $\tau_3(x, z, t)=\mu\partial w'/\partial y|_w$, as well as the wall pressure fluctuations, $p_w(x, z, t)$, are Fourier transformed in the x, z and t directions and the power spectral density, $\Psi(k_1, k_3, \omega)$, is computed. Here, x and z denote the spanwise and axial directions, respectively. k_1 and k_3 denote the spanwise and streamwise wave numbers, which have the ranges of $0\le k_1\le31.5/\delta$, $0\le k_3\le47.5/\delta$ for $\delta/a=2$ and 5, and $0\le k_1\le63.5/\delta$, $0\le k_3\le79.5/\delta$ for $\delta/a=10$. The resolutions are $\Delta k_1=1/\delta$ and $\Delta k_3=1(2\delta)$ for $\delta/a=2$ and 5, and $\Delta k_1=1/\delta$ and $\Delta k_3=1/(3\delta)$ for $\delta/a=10$.

One- and two-dimensional power spectra, $\phi(k_1)$, $\phi(k_3)$, $\phi(\omega)$, $\Phi(k_1, k_3)$ and $\Phi(k_3, \omega)$, are obtained by integrating $\Psi(k_1, k_3, \omega)$ over the remaining one or two variables. Auto-correlation functions are obtained by the inverse Fourier transformation. For example,

$$R(r_z, r_t)=\sum_{k3}\sum_{\omega}\Psi(k_3, \omega)\,e^{ik_3r_3}e^{i\omega r_t} \tag{3}$$

where r_3 and r_t denote the spatial and temporal separations, respectively.

4. Power Spectra

Figures 1~3 show the one-dimensional power spectra of $\tau_1=\mu\partial u'/\partial y|_w$ and $\tau_3=\mu\partial u'/\partial y|_w$ for $\delta/a=2$, 5 and 10. Here each spectrum satisfies the following condition:

$$\int_0^\infty\phi(\omega)\,d\omega=\int_0^\infty\phi(k_1)\,dk_1=\int_0^\infty\phi(k_3)\,dk_3 =\tau_{1rms}^2 \text{ or } \tau_{3rms}^2 \tag{4}$$

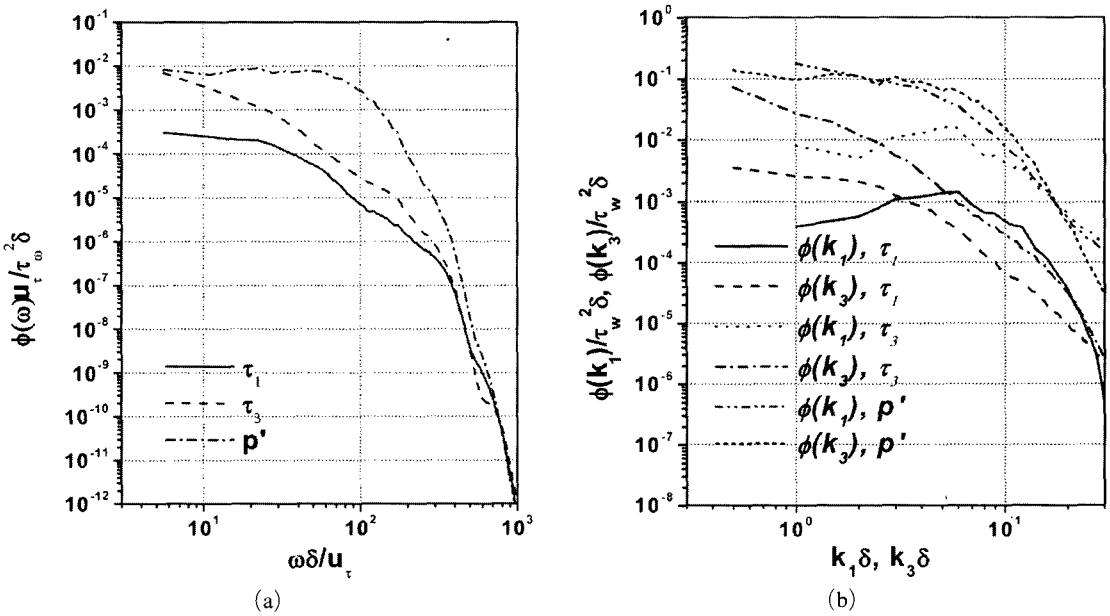

Fig. 1 Spectra of the wall-shear stress fluctuations. (a) frequency (b) stream and spanwise wave numbers. $\delta/a=2$

The frequency power spectrum, $\phi(\omega)$, of τ_1 is nearly constant at low frequencies, while that of τ_3 decreases as the frequency increases [Figs. 1~3(a)]. The streamwise-wave-number piwer spectrum $\phi(k_3)$ has similar characteristics as $\phi(\omega)$ [Figs. 1~3(b)]. The similarity between $\phi(k_3)$ and $\phi(\omega)$ is due to the convective nature of the wall shear-stress fluctuations. On the

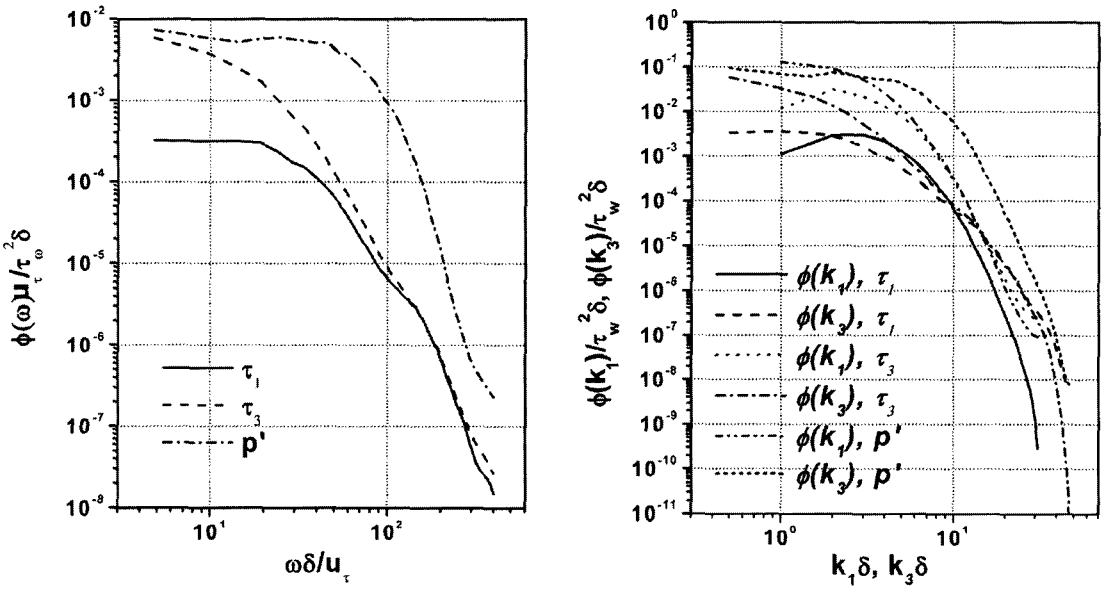

(a) (b)

Fig. 2 Spectra of the wall-shear stress fluctuations. (a) frequency (b) stream and spanwise wave numbers. $\delta/a=5$

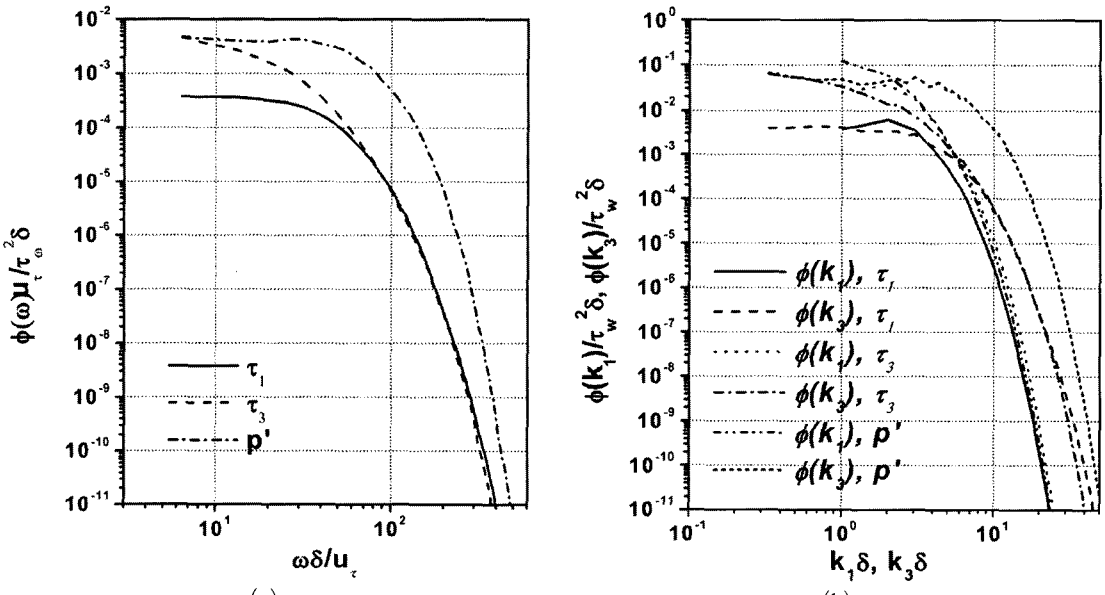

(a) (b)

Fig. 3 Spectra of the wall-shear stress fluctuations. (a) frequency (b) stream and spanwise wave numbers. $\delta/a=10$

other hand, the spanwise-wave-number power spectrum $\phi(k_1)$ is very different from $\phi(\omega)$ and $\phi(k_3)$; $\phi(k_1)$ increases as the wave number increases at low wave numbers. It is also notable that there is a maximum power at $k_1\delta \approx 5$, 2 and 1 for $\delta/a=2$, 5 and 10, respectively. Jeon et al. (1999) reported that the spanwise wave length corresponding to these wave numbers are very close to the mean streak spacing near the wall (Kim et al., 1987; Kline et al., 1967).

At low wave numbers and frequencies, spectra of τ_3 are larger than those of τ_1, but they are nearly the same at high wave numbers and frequencies as δ/a increases, meaning that small scale fluctuations of both τ_1 and τ_3 have almost the same power when large curvature exists. On the hand, for a given flow variable (τ_1 or τ_3), there is more power in $\phi(k_3)$ than in $\phi(k_1)$ at low wave numbers as δ/a decreases. For $\delta/a=10$, power spectra of $\phi(k_3)$ and $\phi(k_1)$ are almost same at low wave numbers. For relatively high wave numbers, $\phi(k_1)$ than in $\phi(k_3)$, indicating that small scale fluctuations in the spanwise direction are more energetic than those in the streamwise direction for small curvature effect but the reverse is true for large curvature effect.

Comparison of the computed power spectrum of τ_3 with the existing experimental and simulation data for flat and axial turbulent boundary layers are provided in Fig. 4. Choi and Moin (1990) showed that the wall pressure spectra of different Reynolds numbers collapse at high frequencies when they are normalized with the inner variables (u_τ and ν), while they collapse at low frequencies when normalized with the outer variables (U_o and δ^*). Here U_o and δ^* are the free-stream velocity and displacement thickness. Figures 4(a) and 4(b) show the normalizations of the spectra $\phi(\omega)$ with the inner and outer variables, respectively, as was done in Choi and Moin (1990); neither normalization produces a collapse like Jeon et al.(1999) reported.

Fig. 5 shows the comparison between the experimental and the simulation data. The experiment is done by one of the authors. It shows that as the momentum Reynolds number increases,

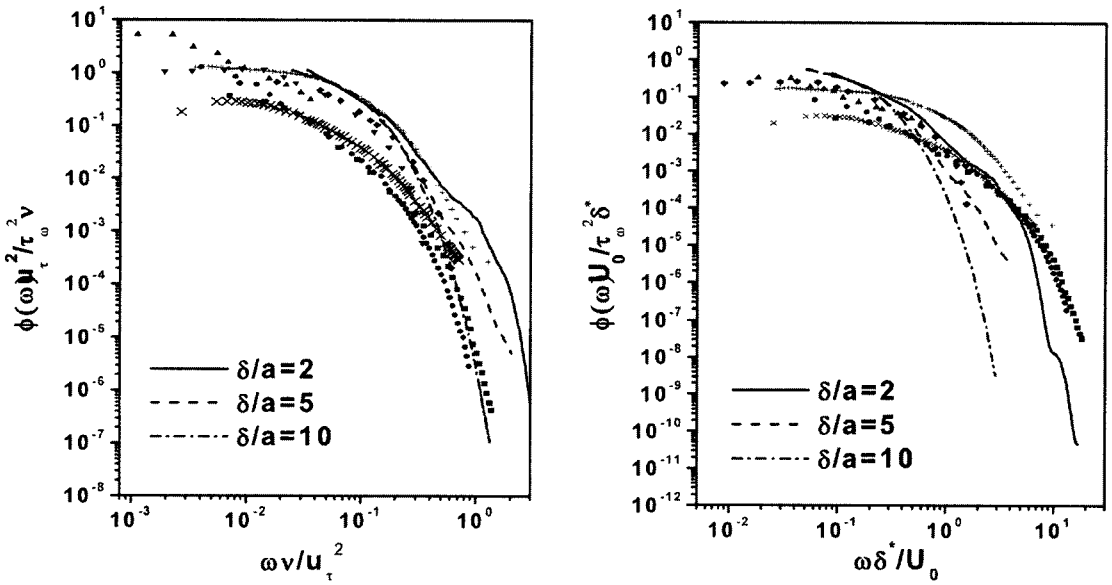

Fig. 4 Frequency spectra of the wall shear-stress fluctuations of τ_3: (a) inner variable scaling; (b) outer variable scaling. ———, $Re_\tau=193$ ($\delta/a=5$, present study); – – – –, $Re_\tau=180$ (Jeon et al., 1999); ▼, $Re_d=289$, (Sreenivasan and Antonia, 1977); ◆, $Re_\tau=554$, (Sreenivasan and Antonia, 1977); +, $Re_\tau=896$ (Wietrzak and Lueptow, 1994); ×, $Re_\tau=1850$ (Yang, 1996); ▲, $Re_\tau=3060$ (Madavan et al., 1985); ■, $Re_\tau=2669$ (Keith and Bennett, 1991); ●, $Re_\tau=3966$ (Keith and Bennett, 1991)

power spectra nomalized by inner variables become larger. The simulation and experimental data agree very well when momentum Reynolds numbers are around 850.

Figure 6 shows the frequency/streamwise wave number spectra of the wall pressure fluctuation. The spectrum $\Phi(k_3, \omega)$ is normalized by its mean square value to satisfy the following condition

$$\int_{-\infty}^{\infty}\int_{-\infty}^{\infty}\Phi(k_3, \omega)\,d\omega dk_3=1 \qquad (5)$$

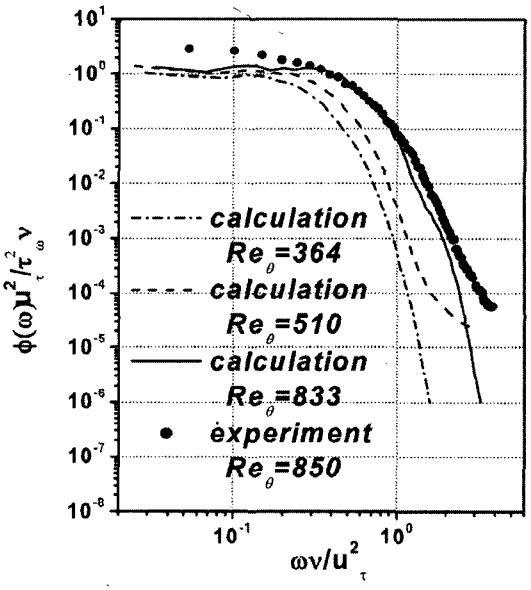

Fig. 5 Comparison of frequency spectra of the wall shear-stress fluctuations of τ_3 normalized by inner variables

Thin band-shaped contours represent strong convective nature of the wall variables. Other flow variables show the similar behavior and there is no noticeable difference with different δ/a.

Figures 7~9 shows the streamwise/spanwise wave number spectra $\Phi(k_1, k_3)$ of the wall flow variables. They are also normalized in the same way as $\Phi(k_3, \omega)$. In general, the contours for all three variables are elongated in the k_1 direction for $\delta/a=2$ like the flat channel flow (Jeon et al., 1999) but they are elongated in the k_3 direction for $\delta/a=10$. It means that more power is distributed in the in the k_1 direction than in the k_3 direction when small curvature effect exists, but the reverse is true when large curvature effect dominates. This is especially true for τ_3 and p_w and the change is moderate for τ_1.

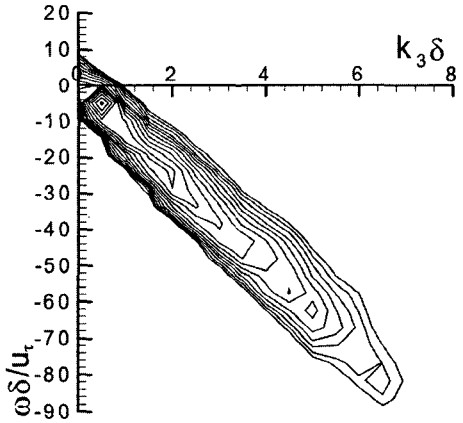

Fig. 6 Contours of $\Phi(k_3, \omega)$ for p_w. $\delta/a=5$. Contour levels are distributed from 10^{-3} to 10^{-6}

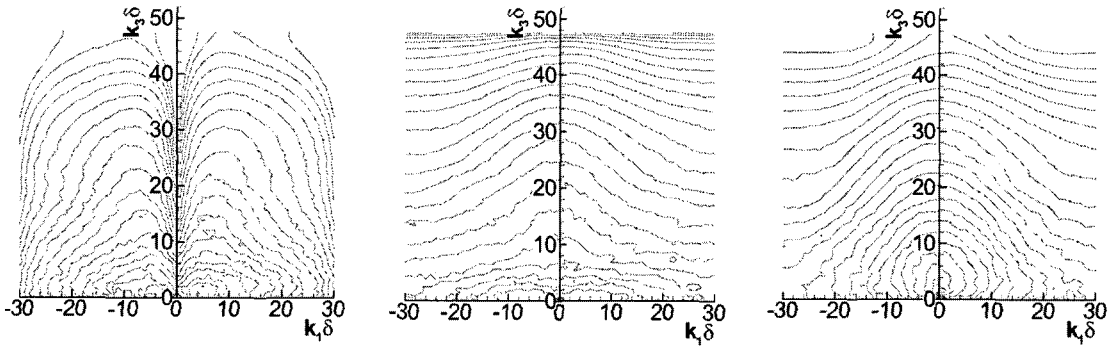

Fig. 7 Contours of $\Phi(k_1, k_3)$: (a) τ_1 (b) τ_3 (c) p_w. $\delta/a=2$

Figure 10 shows the two-point auto-correlations of the wall flow variables as functions of the streamwise and spanwise separations for $\delta/a=5$. The $\delta/a=2$ and 10 cases show similar behavior. It is clearly seen that the spatial distributions of the wall shear-stress fluctuations are very different from that of the wall pressure fluctuations. Negative spanwise correlation occurs for τ_1 and τ_3, but negative streanwise correlation occurs for p_w. Channel flow (Jeon et al., 1999) shows that similar correlation behavior for τ_1 and τ_3 in streamwise direction but negative

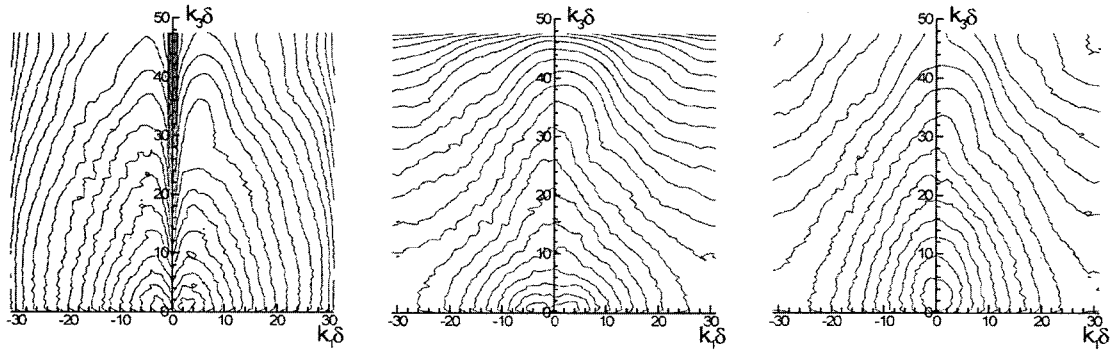

Fig. 8 Contours of $\Phi(k_1, k_3)$: (a) τ_1 (b) τ_3 (c) p_w. $\delta/a=5$

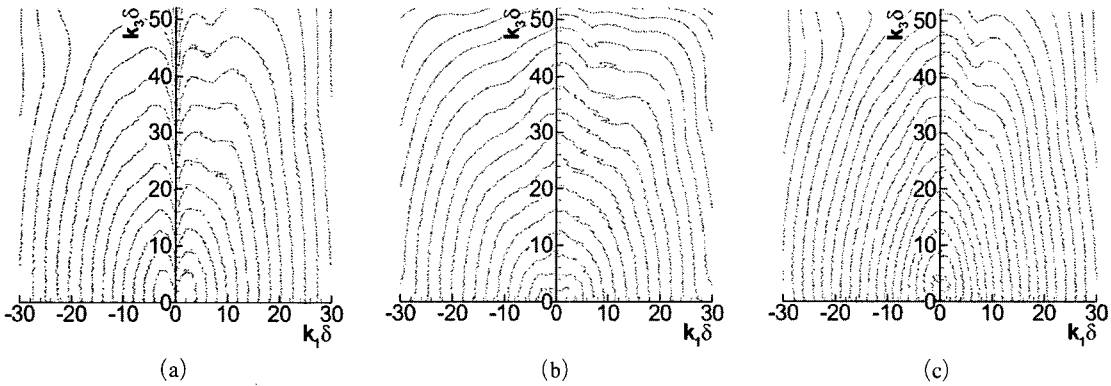

Fig. 9 Contours of $\Phi(k_1, k_3)$: (a) τ_1 (b) τ_3 (c) p_w. $\delta/a=10$

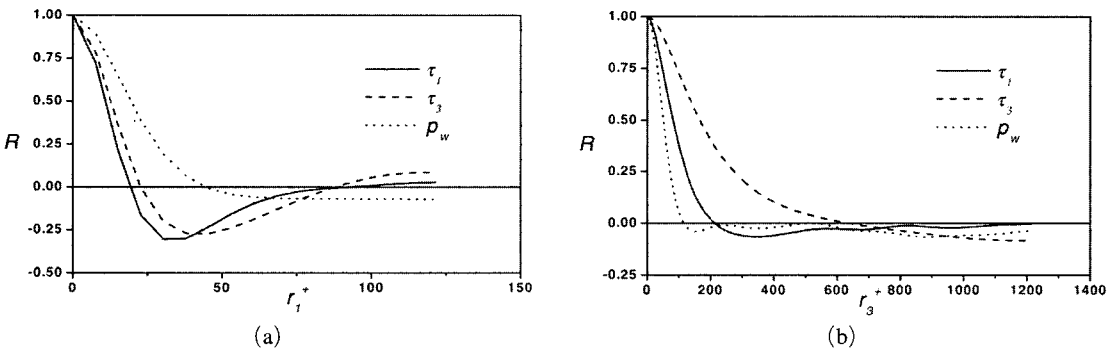

Fig. 10 Two-point auto-correlations as functions of the streamwise and spanwise separation distances: (a) r_1^+ (b) r_3^+. $\delta/a=5$

streamwise correlation for τ_1 occurs where positive streamwise correlation for τ_3 still exists. The negative maximum correlation at $r_3^+ \approx 150$ for p_w and at $r_1^+ \approx 30$ and 40 for τ_1 and τ_3, respectively.

In Fig. 11, contour plots of $R(r_x^+, R_z^+)$ for $\delta/a=5$ are drawn for τ_1, τ_3 and p_w. Here r_x^+ and r_z^+ mean r_1^+ and r_3^+, respectively. The $\delta/a=2$ and 10 cases show similar behavior. The contours for τ_3 are elongated in the streamwise direction due to the streaky structures. There are negative contours in the spanwise direction for τ_1 and τ_3 and in the streamwise direction for p_w and the contours do not show an absolute symmetry. Channel flow (Jeon et al., 1999) also shows similar characteristics.

The two-point correlations $R(r_t^+, r_z^+)$ of the wall flow variables for $\delta/a=5$ are shown in Fig. 12. Here r_z^+ means r_3^+. The $\delta/a=2$ and 10 cases show similar behavior. The strong convective property of the wall flow variables is displayed by the concentration of the contours into narrow bands. Even though the wall pressure fluctuations have the narrowest contour shapes, the contour level for p_w at given r_z^+ and r_t^+ is much lower than that for τ_3. By comparing the correlation values in Fig. 12, it can be deduced that τ_3 has

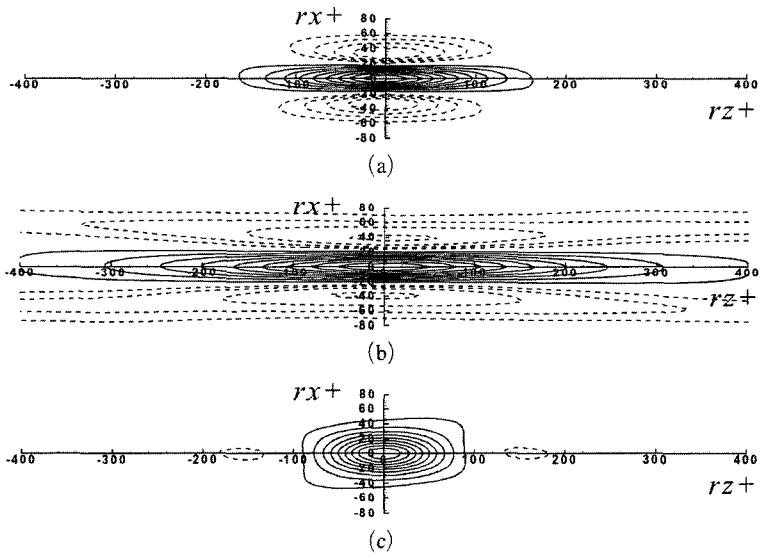

Fig. 11 Contours of two-point auto-correlations $R(r_x^+, r_z^+)=\overline{f(x, z)f(x+r_x^+, z+r_z^+)}/f_{rms}^2$: (a) τ_1 (b) τ_3 (c) p_w. $\delta/a=5$

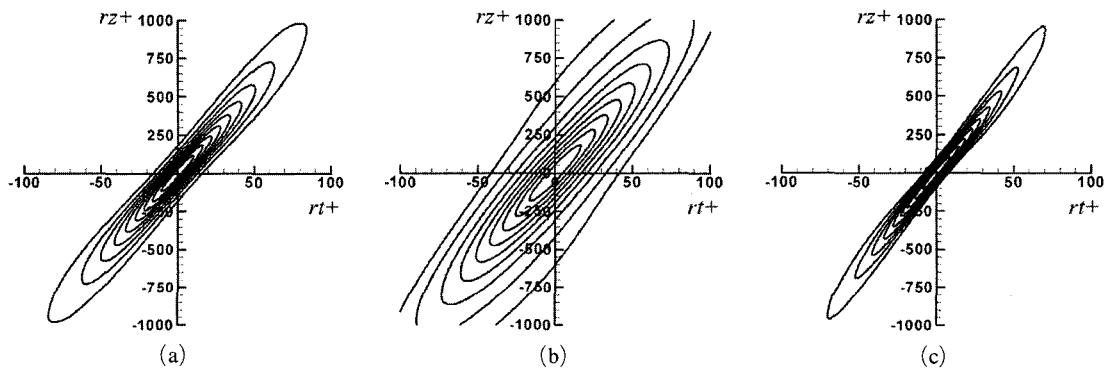

Fig. 12 Contours of $R(r_t^+, r_x^+)=\overline{f(t, x)f(t+r_t^+, z+r_z^+)}/f_{rms}^2$: (a) τ_1 (b) τ_3 (c) p_w. $\delta/a=5$

the strongest convective characteristics. The reason that τ_3 has relatively wide contour shapes is due to its elongated shape in the streamwise direction. It is also interesting to not that the wall pressure correlation has negative contours, while others do not, which is consistent with the behavior of $R(r_x^+, R_z^+)$ at r_x^+ shown in Fig. 11.

5. Summary

The space-time characteristics of the wall shear-stress and pressure fluctuations were investigated using data from direct numerical simulation of axial turbulent boundary layers. The three-dimensional power spectra as a function of the streamwise and spanwise wave numbers and frequency were obtained. It was shown from one-dimensional power spectra that at low wave numbers and frequencies, the power of $\tau_3(x, z, t)=\mu\partial w'/\partial y|_w$ is larger than that of $\tau_1=\mu\partial u'/\partial y|_w$, while the powers of τ_1 and τ_3 are almost the same at high wave numbers and frequencies. The streamwise-wave-number power spectrum $\phi(k_3)$ has similar characteristics as $\phi(\omega)$, which is due to the convective nature of the wall shear-stress fluctuations. It was seen from the power spectra that small scale fluctuations in the spanwise direction have more power than those in the streamwise direction. The streamwise/spanwise wave number spectra, $\Phi(k_1, k_3)$, show that more power is distributed in the k_1 in the direction than in the k_3 direction when small curvature effect exists, but the reverse is true when large curvature effect dominates. The effects are especially true for τ_3 and p_w and the change is moderate for τ_1. In two-point auto-correlations, negative correlation occurs in streamwise separations for p_w, and in spanwise separations for τ_1 and τ_3. the elongated structure of τ_1 in the streamwise direction and the positive and negative pairs of τ_3 in the spanwise direction were demonstrated in one- and two-dimensional correlations.

Acknowledgments

This work has been supported by the Grant No. R01-2004-000-10041-0 from the Basic Research Program of the Korea Science & Engineering Foundation.

References

Blake, W. K., 1986, *Mechanics of Flow-Induced Sound and Vibration*, Academic, London.

Choi, H. and Moin, P., 1990, "On the Space-Time Characteristics of the Wall Pressure Fluctuations," *Phys. Fluids A*, 2, pp. 1450~1460.

Farabee, T. M. and Casarella, M. J., 1991, "Spectral Freatures of Wall Pressure Fluctuations Beneath Turbulent Boundary Layer," *Phys. Fluids A*, 5, pp. 2410~2420.

Jeon, S., Choi, H., Yoo, J. and Moin, P., 1999, "Space-Time Characteristics of the Wall Shear-Stress Fluctuations in a Low-Reynolds-Number Channel Flow," *Phys. Fluids A*, 11, pp. 3084~3094.

Keith, W. L. and Bennett, J. C., 1991, "Low-Frequency Spectra of the Wall Shear Stress and Wall Pressure in a Turbulent Boundary-Layer," *AIAA J.*, Vol. 29, pp. 526~530.

Kim, J. and Choi, H., 2004, "An Immersed-Boundary Finite-Volume Method for Simulation of heat Transfer in Complex Geometries," *KSME International Journal*, Vol. 18, No. 6, pp. 1026~1035.

Madavan, N. K., Deutsch, S. and Merkle, C. L., 1985, "Measurements of Local Skin Friction in a Microbubble-Modified Turbulent Boundary Layer," *J. Fluid Mech.*, Vol. 156, pp. 237~256.

Neves, J. C., Moin, P. and Moser, R. D., 1994, "Effects of Convex Transverse Curvature on Wall-Bounded Turbulence. Part 2 : The Pressure Fluctuations," *J. Fluid Mech.*, 272, pp. 383~406.

Shin, D. S., 2000, "Direct Numerical Simulation of 3-Dimensional Axial Turbulent Boundary Layers with Spanwise Curvature," *KSME International Journal*, Vol. 14, No. 4, pp. 441~447.

Sreenivasan, K. R. and Antonia, R. A., 1977, "Properties of Wall Shear Stress Fluctuations in a Turbulent Duct Flow," *J. Appl. Mech.*, Vol. 44, pp. 389~397.

Wietrzak, A. and Lueptow, R. M., 1994, "Wall Shear Stress and Velocity in a Turbulent Axisymmetric Boundary Layer," *J. Fluid Mech.*, Vol. 239, pp. 191~218.

Yang, J., 1996, "Correlation of the Wall Skin-Friction and Streamwise Velocity Fluctuations in a Turbulent Boundary Layer," *Ph.D. thesis, Dept. of Mechanical Engineering*, Seoul National Univ., Seoul, Korea.